Original Article

Glucose-Induced Reactive Oxygen Species Cause Apoptosis of Podocytes and Podocyte Depletion at the Onset of Diabetic Nephropathy

Katalin Susztak,[1] Amanda C. Raff,[1] Mario Schiffer,[1] and Erwin P. Böttinger[2]

Diabetic nephropathy is the most common cause of end-stage renal disease in the U.S. Recent studies demonstrate that loss of podocytes is an early feature of diabetic nephropathy that predicts its progressive course. Cause and consequences of podocyte loss during early diabetic nephropathy remain poorly understood. Here, we demonstrate that podocyte apoptosis increased sharply with onset of hyperglycemia in $Ins2^{Akita}$ (Akita) mice with type 1 diabetes and $Lepr^{db/db}$ (*db/db*) mice with obesity and type 2 diabetes. Podocyte apoptosis coincided with the onset of urinary albumin excretion (UAE) and preceded significant losses of podocytes in Akita (37% reduction) and *db/db* (27% reduction) mice. Increased extracellular glucose (30 mmol/l) rapidly stimulated generation of intracellular reactive oxygen species (ROS) through NADPH oxidase and mitochondrial pathways and led to activation of proapoptotic p38 mitogen-activated protein kinase and caspase 3 and to apoptosis of conditionally immortalized podocytes in vitro. Chronic inhibition of NADPH oxidase prevented podocyte apoptosis and ameliorated podocyte depletion, UAE, and mesangial matrix expansion in *db/db* mice. In conclusion, our results demonstrate for the first time that glucose-induced ROS production initiates podocyte apoptosis and podocyte depletion in vitro and in vivo and suggest that podocyte apoptosis/depletion represents a novel early pathomechanism(s) leading to diabetic nephropathy in murine type 1 and type 2 diabetic models.
***Diabetes* 55:225–233, 2006**

From the [1]Division of Nephrology, Department of Medicine, Albert Einstein College of Medicine, Bronx, New York; and the [2]Division of Nephrology, Department of Medicine, Mount Sinai School of Medicine, New York, New York

Address correspondence and reprint requests to Erwin Böttinger, Mount Sinai School of Medicine, One Gustave L. Levy Place, New York, NY 10029. E-mail: erwin.bottinger@mssm.edu. Or Katalin Susztak, Albert Einstein College of Medicine, 1300 Morris Park Ave., Bronx, NY 10461. E-mail: ksusztak@aecom.yu.edu.

Received for publication 13 July 2005 and accepted in revised form 22 September 2005.

Additional information for this article can be found in an online appendix at http://diabetes.diabetesjournals.org.

AKT, v-akt murine thymoma viral oncogene homolog; DAPI, 4′-6-diamidino-2-phenylindole; DPI, diphenyl iodonium; ERK, extracellular signal–regulated kinase; ESRD, end-stage renal disease; MAPK, mitogen-activated protein kinase; PAS, periodic acid Schiff; ROS, reactive oxygen species; TGF, transforming growth factor; TTFA, 2-thenoyltrifluoroacetone; TUNEL, transferase-mediated dUTP nick-end labeling; UAE, urinary albumin excretion; WT-1, Wilms tumor antigen-1.

Diabetic nephropathy is a serious and common complication of type 1 and type 2 diabetes leading to end-stage renal disease (ESRD) in up to 30% of individuals with diabetes (1). The natural history of diabetic nephropathy has been delineated in particular in type 1 diabetes (2–4). A latent period of several years after onset of diabetes is characterized by increased glomerular filtration rate without overt clinical signs and symptoms. The first manifestation of diabetic nephropathy in humans is increased urinary albumin excretion, which usually progresses to nephrotic-range proteinuria. The morphological substrates for these functional abnormalities of the glomerular filter apparatus include glomerular hypertrophy, thickening of glomerular basement membrane, and expansion of mesangial extracellular matrix. Advanced diabetic nephropathy is characterized by glomerulosclerosis, demise of glomerular capillaries, tubulointerstitial degeneration, and fibrosis associated with precipitous decline of glomerular filtration rate (5). To date, several interventions have been shown to slow the progression of diabetic nephropathy, including tight glucose and blood pressure control and blockade of the renin-angiotensin system (6–10). However, none of the currently available modalities can cure or prevent diabetic nephropathy.

Several factors have been shown to influence the progression of diabetic nephropathy after onset of albuminuria; transforming growth factor (TGF)-β, angiotensin II, and advanced glycated proteins have been extensively characterized (11–13). These factors are thought to converge and to promote glomerular and tubular fibrogenesis. In contrast, very little is known about the cellular and molecular pathomechanisms that initiate diabetic nephropathy and that precede the onset of clinical albuminuria. Detailed morphometric analyses of protocol renal biopsies were obtained after the onset of diabetes but before manifestations of diabetic nephropathy in individuals with type 1 and type 2 diabetes (2,5,14,15). These seminal studies demonstrate that the density of glomerular visceral epithelial cells is reduced in kidneys of individuals with diabetic nephropathy and also in patients with short duration of diabetes without evidence of diabetic nephropathy (11,15). Among various glomerular morphological characteristics, the decreased number of podocytes per glomerulus was the strongest predictor of progression of diabetic nephropathy, where fewer cells predicted more rapid progression (14,15). Although these observations identify podocyte depletion as one of the earliest cellular

features of human diabetic nephropathy, the course, consequences, molecular pathways, and pathomechanism(s) that underlie the loss of podocytes in diabetic nephropathy remain poorly understood.

Recent studies in streptozotocin-induced diabetic rats suggest that podocytes may detach from glomerular basement membrane leading to loss of podocytes into the urinary space (16). These investigators were able to culture cells expressing typical podocyte protein markers from urine, indicating that some podocytes may remain viable after detachment (17,18). Apoptosis of resident glomerular podocytes has recently been proposed as a cellular mechanism that may underlie podocyte loss in nondiabetic glomerulopathies characterized by progression to glomerulosclerosis (19). For example, progressive glomerulosclerosis in TGF-β1 transgenic mice (20) and CD2AP$^{-/-}$ mice (21) is associated with early increases of podocyte apoptosis and subsequent progressive podocyte depletion. Interestingly, podocyte apoptosis precedes endocapillary and tubular epithelial apoptosis in these models. Apoptosis of glomerular cells, in particular of podocytes, has not yet been documented in human or experimental diabetic nephropathy. Moreover, it is not known whether podocyte apoptosis and depletion initiate and/or contribute to albuminuria and mesangial expansion—hallmarks of human and experimental diabetic nephropathy.

Here, we demonstrate for the first time that high extracellular glucose induces reactive oxygen species (ROS) production, activation of proapoptotic p38 mitogen-activated protein kinase (MAPK), and apoptosis of cultured podocytes. In murine type 1 and type 2 diabetic models, podocyte apoptosis precedes podocyte depletion, urinary albumin excretion (UAE), and mesangial matrix expansion, suggesting that podocyte apoptosis/depletion represents a novel early pathomechanism leading to diabetic nephropathy. NADPH oxidase is a key mediator of podocyte apoptosis and subsequent diabetic glomerulopathy in vivo, thus mechanistically linking hyperglycemia, ROS, podocyte apoptosis, podocyte depletion, and diabetic nephropathy.

RESEARCH DESIGN AND METHODS

Apocynin, 3-nitropropionate, 2-thenoyltrifluoroacetone (TTFA), myxothiazol, and diphenyl iodonium (DPI) were purchased from Sigma (St. Louis, MO).

As type 2 diabetic models, we used male *db/db* (*Lepr*$^{db/db}$) mice together with nondiabetic control *db/m* on C57BLKs/J background (The Jackson Laboratories, Bar Harbor, ME). Apocynin treatment was initiated at 5 weeks of age (*db/db* and *db/m* mice) at 2.4 g/l concentration dissolved in sterile water that was sweetened with NutraSweet. The average consumption was 30 mg/kg. The dose of apocynin was based on prior in vivo studies of prolonged dosing in which apocynin in the dosing of 4–100 mg/kg prevented NADPH oxidase activation, vascular superoxide production and remodeling, hypertension, inflammation and/or organ dysfunction, and diabetic neuropathy (22–24). As a type 1 diabetic model, we used male and female Akita (C57B6J/Ins2^{Akita}) mice together with nondiabetic control C57B6/J mice. All mice were maintained on normal mouse chow (5001Rodent Chow; Purina, Quakertown, PA). All animal protocols and procedures were approved by the institutional animal care and use committee at the Albert Einstein College of Medicine and at the Mount Sinai School of Medicine.

For determination of urinary albumin excretion, mice were placed in individual metabolic cages (Nalgene, Rochester, NY), and urine was collected for 24 h. Urinary albumin was measured using an ELISA specific for mouse albumin (Albuwell; Exocell, Philadelphia, PA), and urine creatinine was determined using Creatinine Companion (Exocell). Blood glucose was measured using Glucometer Elite.

Immunohistochemistry. For analysis of glomerular histology, formalin-fixed, paraffin-embedded kidney tissue sections were stained with periodic acid Schiff (PAS) reagent. Mesangial matrix expansion was evaluated semi-quantitatively on 35–50 glomeruli per kidney, using a score of 1 for minimal, 2 for mild mesangial matrix expansion, 3 for moderate, and 4 for diffuse, mesangial matrix expansion. Podocyte number was determined on 4-μm frozen sections double stained with Wilms tumor antigen-1 (WT-1) (1:50; rabbit polyclonal) (Santa Cruz Biotechnology, Santa Cruz, CA) and synaptopodin (G1; mouse monoclonal). Cells stained positive for both synaptopodin and WT-1 were counted on all the glomeruli (35–50) on the transverse section of the left kidney (20,21).

Scoring of apoptotic nuclei in situ. Apoptotic nuclei were detected by a transferase-mediated dUTP nick-end labeling (TUNEL) assay of kidney sections using peroxidase and counterstaining with hematoxylin and PAS stain, as described previously (20,21). The TUNEL assay was used according to the manufacturer's protocol (Chemicon, Temecula, CA). Positive cells were counted as podocytes when residing on the outer aspect of PAS-positive basement membrane. Cells residing in areas circumscribed by PAS-positive basement membrane were counted as endocapillary/mesangial cells.

Cell culture. Cultivation of conditionally immortalized mouse podocytes was performed as reported previously (25). Briefly, cells were grown on type 1 collagen (BD Bioscience, Bedford, MA) at 33°C in the presence of 20 units/ml interferon-γ (Invitrogen, Carlsbad, CA) in RPMI 1640 (Mediatech, Herndon, VA) containing 10 mmol/l glucose, 10% FCS, and antibiotics. To induce differentiation, podocytes were maintained at 37°C without interferon for 10 days. Cells were growth arrested in RPMI 1640 containing 0.2% serum and 5 mmol/l D-glucose for 24 h before the experiment.

Apoptosis detection. Apoptotic nuclei were detected using 4′-6-diamidino-2-phenylindole (DAPI) (Sigma) staining (1 μg/ml; 10 min) in cultured cells fixed with 4% paraformaldehyde and analyzed via fluorescence microscopy to assess chromatin condensation and segregation. Caspase 3 activity was detected by using the ApoAlert Caspase3 Fluorescent Detection system (DB Bioscience), according to the manufacturer's protocol. Activity was normalized to total protein content.

Determination of ROS generation. ROS generation was measured with the fluoroprobe carboxymethyl-H_2-dichlorofluorescein diacetate (Invitrogen). Briefly, podocytes were incubated for 45 min at 37°C with 10 μmol/l carboxymethyl-H_2-dichlorofluorescein diacetate in PBS, then cells were washed and scraped, and emitted fluorescence was determined by Wallac Victor^2 Fluorescence Plate Reader (PerkinElmer, Wellesley, MA).

Western blotting. Cells were lysed in radioimmunoprecipitation assay buffer containing protease and phosphatase inhibitors as previously described (21). Lysates (30 μg/lane) were subjected to 10% SDS-PAGE before transfer to polyvinylidene difluoride membranes. The following primary antibodies were used for antigen detection: mouse monoclonal anti–total v-akt murine thymoma viral oncogene homolog (AKT)1 (Santa Cruz Biotechnology), rabbit polyclonal anti-S(P)^{475} AKT, mouse anti–phospho–extracellular signal–regulated kinase (ERK)1/2, rabbit anti–total ERK1/2, and rabbit anti–phospho-p38 (all from Cell Signaling [Beverly, MA]).

Statistical methods. Data are reported as means and SE for continuous variables. All cell culture experiments were performed at least three times and summarized. Standard software packages (SPSS and Excel for Windows) were used to provide descriptive statistical plots (unpaired *t* tests). The Bonferroni correction was used for multiple comparisons. An asterisk denotes $P < 0.05$.

RESULTS

Onset of diabetes initiates podocyte loss (depletion) in murine models of type 1 (Akita) and type 2 (*db/db*) diabetes. To determine whether diabetes induces podocyte depletion and to delineate a temporal relationship between onset of diabetes, albuminuria, and changes of podocyte numbers, we subjected two genetic models of experimental diabetes, including Akita (type 1 diabetes) (26,27) and *db/db* (type 2 diabetic) mice (26–28) to standardized phenotype analysis following protocols established by the Animal Models of Diabetic Complications Consortium (www.amdcc.org). Blood glucose levels were not different in C57BL/6J, *db/m*, Akita mice at 2 weeks of age and *db/db* mice at 4 weeks of age (Fig. 1*A* and *D*). Glucose levels were significantly elevated in 4-week-old Akita and 8-week-old *db/db* mice and remained persistently elevated at >500 mg/dl in all diabetic animals until termination of the study at 28 weeks of age (Fig. 1*A* and *D*).

Average numbers of podocytes per glomerular cross

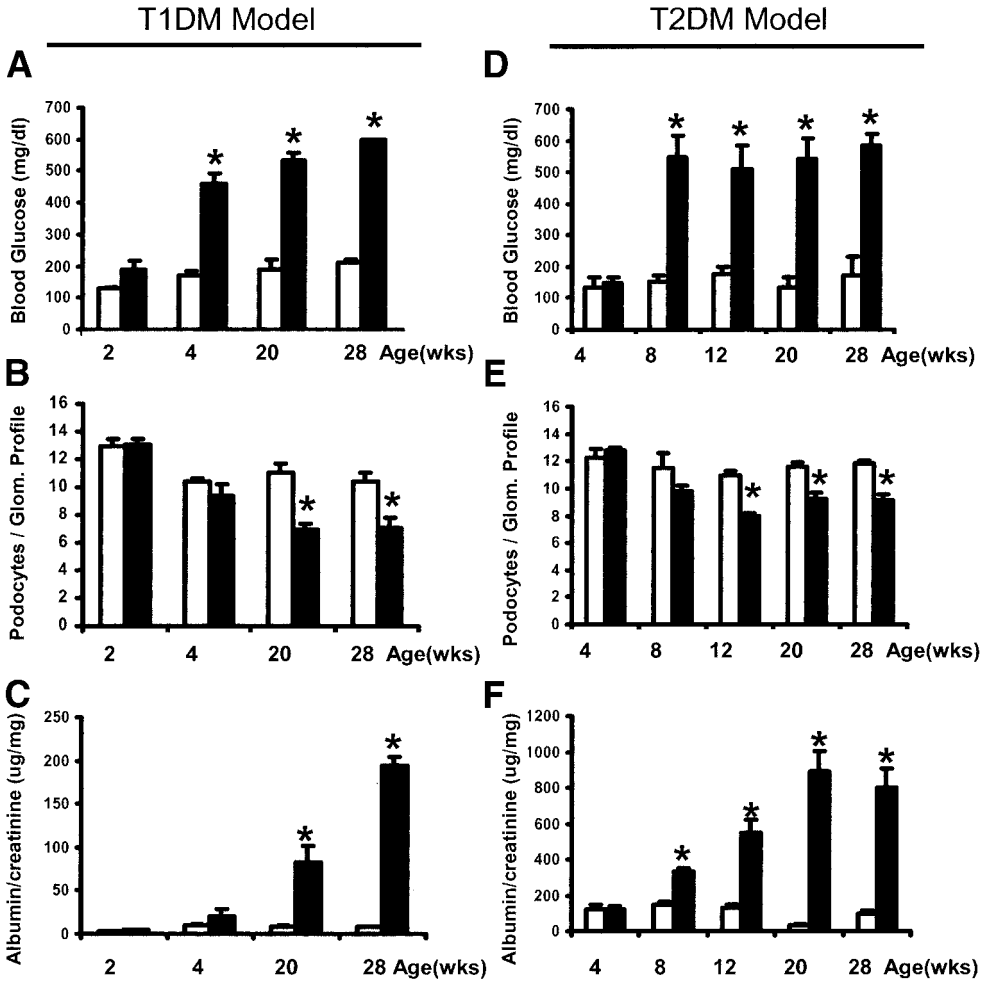

FIG. 1. Serum glucose, podocyte density, and albuminuria in diabetic mouse models. Bars represent means ± SE of measurements of serum glucose (*A* and *D*), podocyte number per glomerular section (*B* and *E*), and urinary albumin-to-creatinine ratio (μg/mg) (*C* and *F*) in nondiabetic control C57BL6/J (□) and type 1 diabetic (T1DM) Akita (■) mice (*A–C*) and in nondiabetic control *db/m* (□) and type 2 diabetic (T2DM) *db/db* (■) mice (*D–F*). Five to 10 mice were analyzed per each genotype of each age-group. **P* < 0.05.

section were determined by counting cells that labeled positive with two podocyte markers, including synaptopodin and WT-1 (21). Before the onset of hyperglycemia, counts of double-positive podocytes were similar (12–13 cells/glomerular profile) in C57BL/6J and Akita mice at 2 weeks of age, as well as *db/m* and *db/db* mice at 4 weeks of age (Fig. 1*B* and *E*). With onset of diabetes, double-positive cell counts tended to decrease in Akita compared with control C57BL/6J at 4 weeks of age (Fig. 1*B*) and in *db/db* compared with *db/m* control at 8 weeks of age (Fig. 1*F*). The decrease was statistically significant by 12 weeks of age in *db/db* mice (26.6% decrease compared with *db/m*; $P < 0.05$) and by 20 weeks of age in Akita mice (37% decrease compared with C57BL/6J; $P < 0.01$). Interestingly, double-positive cell counts remained stable at reduced levels after the initial decline, despite persistent, severe hyperglycemia. Similar results were obtained if we normalized podocyte number per glomerular profile to the mean glomerular volume (Supplemental Tables 1 and 2, which appear in the online appendix [available at http://diabetes.diabetesjournals.org]). UAE rates were measured as the ratio of albumin to creatinine excretion (μg/mg) in 24-h urine collections using metabolic cages. UAE rates tended to increase at 4 weeks and were significantly increased at 10 (not shown), 20, and 28 weeks of age in Akita mice compared with C57BL/6J (Fig. 1*C*). Similarly, UAE were significantly increased at 8, 12, 20, and 28 weeks of age in *db/db* mice compared with *db/m* controls (Fig. 1*E*). Together, these results demonstrate that podocyte counts per glomerular section decrease significantly by ~27–37% after onset of diabetes in type 1 and type 2 diabetic murine models, respectively. On a temporal scale, podocyte loss tracks with the increase in UAE.

A sharp increase of podocyte apoptosis coincides with onset of diabetes and precedes podocyte loss and UAE in Akita and *db/db* mice. Next, we quantitated rates of podocyte apoptosis using TUNEL immunoperoxidase staining in combination with PAS staining to demarcate glomerular basement membrane as previously described (21). Counts of TUNEL-positive podocytes per glomerular profiles were significantly increased in 4-week-old Akita mice compared with age-matched control C57BL/6J mice (0.054 ± 0.005 vs. 0.015 ± 0.005, $P < 0.05$) (Fig. 2*A*). In the *db/db* model, TUNEL-positive podocytes per glomerular section were significantly increased at 8 weeks of age compared with nondiabetic *db/m* (0.055 ± 0.017 vs. 0.011 ± 0.007, $P < 0.05$) (Fig. 2*B*). In both models, Akita and *db/db*, TUNEL-positive podocyte counts were not significantly different between diabetic mice and nondiabetic controls at later time points (Fig. 2*A* and *B*), indicating that a subpopulation of podocytes is susceptible initially, whereas the majority of podocytes adapt to hyperglycemia and become resistant to diabetes-induced apoptosis. Interestingly, counts of apoptotic endocapillary cells were not significantly different between control *db/m* and diabetic *db/db* mice (Fig. 2*C*) or control C57BL6/J and Akita mice (data not shown). Similarly, apoptosis rates of tubular epithelial and interstitial cells were not signifi-

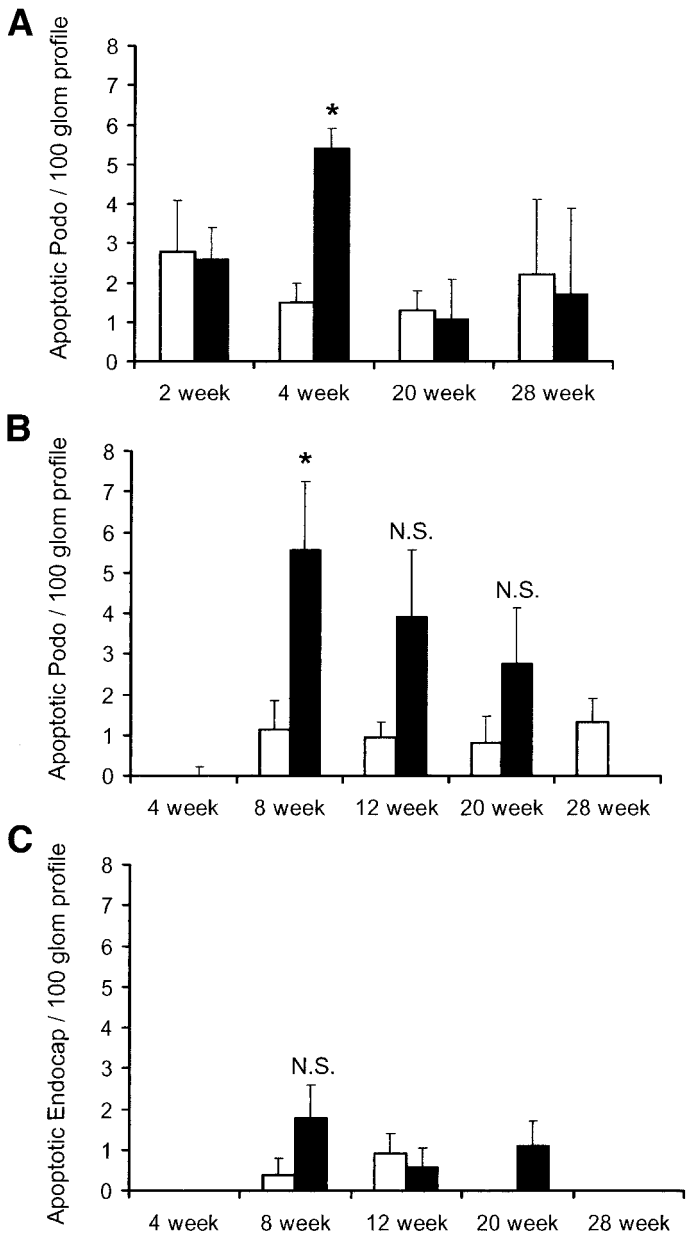

FIG. 2. Quantitative analysis of glomerular apoptosis in diabetic mouse models. *A*: Bar graphs show the mean number of TUNEL-positive podocytes per glomerular profiles in control C57B6J (□) and diabetic Akita (■) mice. *B* and *C*: The mean number of apoptotic podocytes (*B*) and endocapillary cells (*C*) per glomerular cross section in kidneys of *db/db* (■) and *db/m* (□) mice. Five to 10 mice were analyzed per each genotype of each age-group. *$P < 0.05$. NS, not significant.

cantly different (data not shown) (29). Taken together, these observations demonstrate that podocytes are selectively susceptible to diabetes-induced apoptosis and that the onset of diabetes was characterized by a sharp increase in apoptotic podocytes in type 1 and type 2 diabetic mice. On a temporal scale, this "wave" of diabetes-induced podocyte apoptosis was followed by significant podocyte depletion and UAE. As rates of podocyte apoptosis normalized, podocyte loss subsided and podocyte counts per glomerular section stabilized at a significantly lower level compared with nondiabetic controls in both models, suggesting that podocyte depletion depended on podocyte apoptosis in diabetic mice.

Increased extracellular glucose is sufficient to trigger apoptosis of podocytes in vitro through increased synthesis of ROS. We observed increased podocyte apoptosis in vivo within days of onset of diabetes in Akita and *db/db* mice, suggesting that metabolic factors may provide a proapoptotic stimulus. We subjected conditionally immortalized murine podocytes, maintained under permissive (33°C; interferon-γ) or nonpermissive, differentiated conditions (37°C; no interferon-γ for 10 days), respectively, to increasing glucose concentrations in the culture medium, ranging from 5 (baseline) to 30 mmol/l. Increased extracellular glucose was sufficient to induce apoptosis in podocytes maintained under permissive or nonpermissive conditions in a dose-dependent manner (Fig. 3*A* and *B*). In addition, high glucose was sufficient to increase significantly caspase 3 activity in differentiated podocytes within 3 h of treatment (Fig. 3*C*), and the response was also dose dependent (Fig. 3*D*). These results demonstrate that increased extracellular glucose concentration was sufficient to induce podocyte apoptosis in vitro, irrespective of the state of podocyte cell growth or podocyte differentiation.

Previous studies demonstrated that intracellular ROS mediate apoptosis of mesangial cells, cardiac myocytes, and dorsal root ganglion cells induced by hyperglycemia (30–32). We found that ROS generation was significantly and rapidly increased in cultured podocytes in response to increased extracellular glucose (Fig. 4*A*). To determine whether plasma membrane NAPDH oxidase, the mitochondrial pathway, or both were responsible for intracellular ROS generation, we exposed podocytes to high glucose in the presence of various chemical inhibitors of these ROS synthesis pathways. Myxothiazol inhibits the mitochondrial respiratory chain at cytochrome b-c1, and TTFA is an inhibitor of mitochondria electron transport chain complex II. Mitochondrial electron chain blocker myxothiazol and TTFA and the inhibitors of NADPH oxidase, apocynin, and DPI each completely abolished the increase of intracellular ROS induced by high glucose (Fig. 4*B*). Consistent with previous report, we confirmed mRNA expression (by quantitative RT-PCR) of the key components of NADPH oxidase, Nox4, and p22phox in our cultured podocytes (data not shown) (33,34). Thus, our results demonstrate that high ambient glucose induces ROS synthesis in cultured murine podocytes through plasma membrane NADPH oxidase and mitochondrial ROS pathways.

Next, we wished to determine whether increased ROS generation was required for induction of apoptosis in podocytes by high ambient glucose. When podocytes were treated with 30 mmol/l glucose in the presence of the general ROS scavenger tempol, glucose-induced apoptosis was completely abolished (Fig. 4*C*). Similarly, inhibition of mitochondrial ROS generation with electron transport chain inhibitors myxothiazol and TTFA and inhibition of NADPH oxidase with apocynin prevented podocyte apoptosis induced by 30 mmol/l glucose (Fig. 4*C*). Taken together, these findings demonstrate that high ambient glucose is sufficient to induce podocyte apoptosis by increasing ROS synthesis through activation of both plasma membrane NADPH oxidase and mitochondrial ROS generation.

To begin to characterize intracellular signaling mechanisms associated with podocyte apoptosis induced by high ambient glucose, we stimulated podocytes with 30 mmol/l D-glucose for various time intervals and analyzed phosphorylation of proapoptotic and antiapoptotic mediators

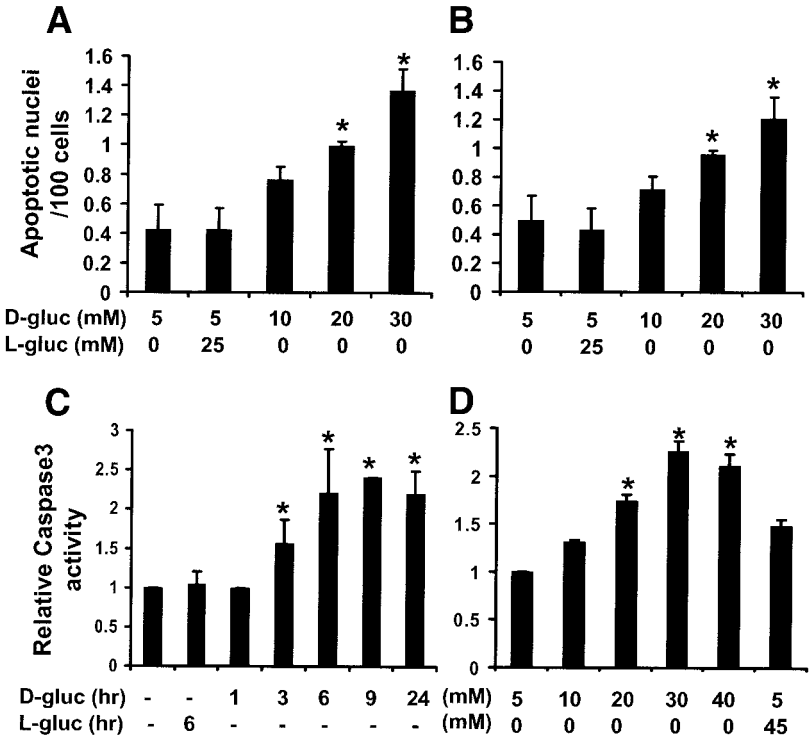

FIG. 3. Increased apoptosis rate in in vitro–cultured murine podocytes incubated in 30 mmol/l D-glucose. Nuclear condensation was quantified via DAPI staining at increasing concentration of D-glucose (5, 10, 20, and 30 mmol/l) in undifferentiated podocytes (*A*) and differentiated podocytes (*B*). Caspase3 activity was measured via DB ApoAlert Caspase3 Fluorescent Assay kit at different time points in differentiated podocytes (*C*) and at increasing concentration of extracellular D-glucose (*D*) after 18 h of treatment. *$P < 0.05$.

(Fig. 5). P38 MAPK mediates proapoptotic signaling and is required for TGF-β–induced podocyte apoptosis (20). High glucose stimulated a strong increase in phosphorylated p38 in podocytes after 1–2 h incubation (Fig. 5). In contrast, glucose treatment had no significant effect on antiapoptotic phospho-AKT levels and caused a moderate but transient increase of phospho-ERK1/2 MAPK (Fig. 5), whereas the total unphosphorylated ERK and AKT levels were not affected. These results suggest that activation of proapoptotic p38 MAPK pathway is associated with podocyte apoptosis induced by high ambient glucose.

Systemic inhibition of NADPH oxidase prevents podocyte apoptosis, reduces loss of podocytes, and ameliorates UAE and mesangial matrix expansion in vivo in *db/db* mice. We demonstrated that apocynin, a specific inhibitor of the plasma membrane NADPH oxidase, prevented ROS generation and apoptosis induced by high ambient glucose in cultured podocytes in vitro (see Fig. 4). To determine the functional significance of NADPH oxidase and its dependent ROS load in podocyte apoptosis and podocyte depletion associated with type 2 diabetes in *db/db* mice, we treated *db/m* control and *db/db* animals with apocynin starting at 5 weeks of age, before onset of diabetes. No significant toxicity was observed in the animals treated with apocynin. As expected, podocyte apoptosis, assessed by TUNEL staining, was significantly increased at 8 weeks of age in *db/db* animals treated with vehicle control compared with nondiabetic *db/m* mice (Fig. 6*A*). In contrast, treatment with apocynin in drinking water significantly reduced podocyte apoptosis in *db/db* mice to levels that were comparable with nondiabetic *db/m* control mice (Fig. 6*A*). Thus, NADPH oxidase–dependent ROS generation constitutes a major mediator of podocyte apoptosis in diabetic mice. Next, we quantitated podocyte counts per glomerular section by synaptopodin/WT-1 double labeling in 20-week-old *db/db* mice. As expected, podocyte counts were significantly decreased (27.65% reduction) in vehicle-treated *db/db* mice compared with *db/m* control (8.05 ± 0.72 vs. 11.2 ± 1.5; $P < 0.05$) (Fig. 6*B*). In contrast, in *db/db* mice treated with apocynin, we detected 9.9 ± 0.4 podocytes per glomerular section (11.25%) reduction (Fig. 6*B*). This result was significantly different from vehicle-treated *db/db* mice ($P < 0.05$), indicating that inhibition of NADPH oxidase significantly reduced the loss of podocytes observed in *db/db* mice after 12 weeks of diabetes. Blood glucose levels were not different between vehicle-treated and apocynin-treated *db/db* mice (Fig. 6*C*). In addition, UAE was significantly reduced in apocynin-treated *db/db* mice compared with vehicle-treated control *db/db* mice (1,036 ± 180 vs. 401 ± 75 μg/mg) (Fig. 6*D*). Taken together, our results demonstrate that the sharp increase in podocyte apoptosis observed during early stages of diabetes in *db/db* mice is mediated to a large extent by activation of NADPH oxidase and its contribution to generation of ROS. Moreover, NADPH oxidase–dependent/ROS-mediated podocyte apoptosis contributes significantly to the subsequent loss of podocytes in diabetic *db/db* mice, accounting for 60% of total podocyte loss. Interestingly, the rate of reduction of podocyte depletion achieved by NADPH oxidase blockade was tightly associated with an ~60% reduction of UAE.

db/db mice are characterized by considerable mesangial matrix expansion after 12 weeks of diabetes (28,35). Mesangial expansion was determined using semiquantitative scoring on PAS section by two independent investigators who were blinded to the origin of the samples (Fig. 7). Scores from both investigators were highly consistent, as determined by correlation of coefficient of 0.75. Therefore, we used the average of both scores from each animal for statistical analysis (Fig. 7*D*). Mesangial expansion scores were significantly increased in vehicle-treated *db/db* (Fig. 7*A*) compared with *db/m* control (Fig. 7*C*) animals (3.00 ± 0.17 vs. 1.37 ± 0.11; $P < 0.001$). In contrast, Mesangial expansion scores were not significantly different between apocynin-treated *db/db* (Fig. 7*B*) and *db/m* (Fig. 7*C*) mice (1.68 ± 0.1 vs. 1.38 ± 0.1; $P = 0.07$) and were significantly

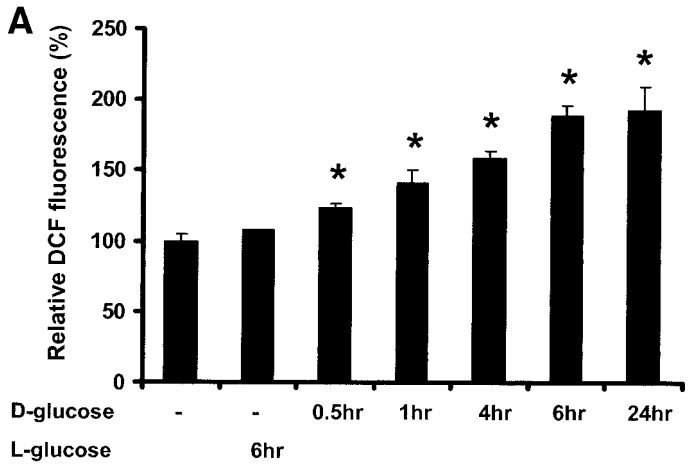

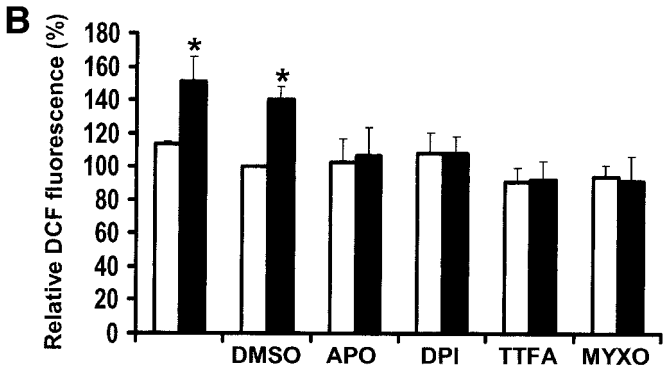

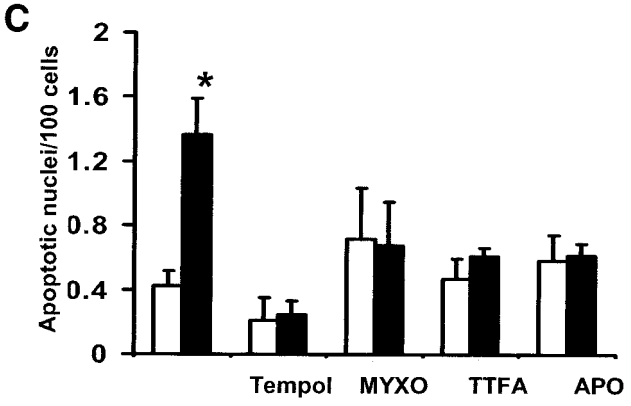

FIG. 4. Podocytes incubated in high-glucose medium generate an increased amount of ROS that is important in the hyperglycemia-induced apoptosis of murine podocytes. *A*: Intracellular ROS release in podocytes was quantified via the changes of DCF (2′-7′-dichlorodihydrofluorescein) fluorescence incubated in 30 mmol/l glucose for various time periods (0.5–24 h) or in the presence of 30 mmol/l L-glucose for 6 h. *B*: ROS generation was examined in the presence of inhibitors apocynin (50 μmol/l), DPI (10 μmol/l), TTFA (10 μmol/l), and myxothiazol (3 μmol/l). Cells were incubated for 1 h at 37°C with the above-mentioned inhibitor before stimulation with 30 mmol/l D-glucose for 4 h. *C*: Podocyte apoptosis was evaluated via DNA condensation on DAPI staining. Podocytes were incubated for 1 h at 37°C with tempol (1 mmol/l), apocynin (50 μmol/l), TTFA (10 μmol/l), and myxothiazol (3 μmol/l) before stimulation with 30 mmol/l D-glucose. □, control; ■, 30 mmol/l D-glucose. *$P < 0.05$.

reduced comparing vehicle-treated and apocynin-treated *db/db* mice (Fig. 7*B*) (3.00 ± 0.17 vs. 1.68 ± 0.1; $P < 0.0001$). These results demonstrate that long-term inhibition of NADPH oxidase significantly ameliorates chronic functional (UAE) and morphological glomerular defects induced by chronic diabetes in *db/db* mice. Thus, reduction of NADPH oxidase–generated ROS load prevented early podocyte apoptosis and was associated with significantly reduced podocyte depletion, UAE, and mesangial expansion at later stages of diabetes-induced glomerulopathy in *db/db* mice.

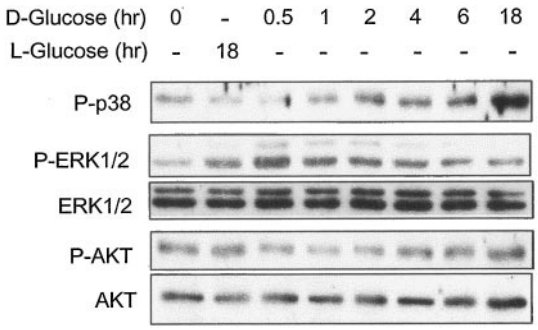

FIG. 5. Activation profiles of signaling mediators induced by hyperglycemia in immortalized murine podocytes. Western blot analysis demonstrates levels of total and phosphorylated p38 and p42/44 MAPK and AKT levels as indicated in total cell protein lysates of conditionally immortalized podocytes after treatment with D-glucose for 30 min and 1, 2, 4, 6, and 18 h or with L-glucose for 18 h.

DISCUSSION

Based on in vivo and in vitro evidence presented in this report, we propose that podocyte apoptosis is a new cellular pathomechanism of diabetic glomerulopathy. We found that podocyte apoptosis coincides with the onset of diabetes/hyperglycemia in two murine models of type 1 and type 2 diabetes where it precedes significant levels of UAE, podocyte depletion, and mesangial matrix expansion. We conclude that podocyte apoptosis may represent one of the earliest cellular lesions affecting the diabetic kidney.

Importantly, our findings are consistent with seminal clinical studies demonstrating that glomerular podocyte density is decreased in type 1 diabetic patients even after short duration of diabetes and before albuminuria (36). Moreover, the extent of podocyte depletion is a top predictor of progression of diabetic nephropathy in Pima Indians affected by type 2 diabetes (14,15). Although these clinical studies clearly demonstrate the phenomenon of podocyte depletion in human diabetic kidney, they cannot address its underlying mechanism(s). There has been little progress in our understanding of mechanisms of early diabetic nephropathy for several reasons. First, tissue from human diabetic kidney is not available because renal biopsies are currently not routinely performed for diagnostic or research purposes in diabetic patients. Second, quantitative and statistical analysis of podocyte apoptosis in archival tissue from human diabetic kidneys is hampered by the limited number of glomerular sampling in biopsy cores and because of the transient, noncumulative nature of cellular apoptosis detection in situ. In this context, we believe that our studies in well-established experimental models are particularly significant because we identify podocyte apoptosis as a new candidate mechanism for podocyte depletion in human diabetic nephropathy that could otherwise not have been detected.

Podocytes are highly specialized cells that control the glomerular filtration apparatus and maintain the structural integrity of the glomerular capillary loops. Apoptosis of podocytes has been demonstrated in various murine models of nondiabetic renal disease: in immune complex

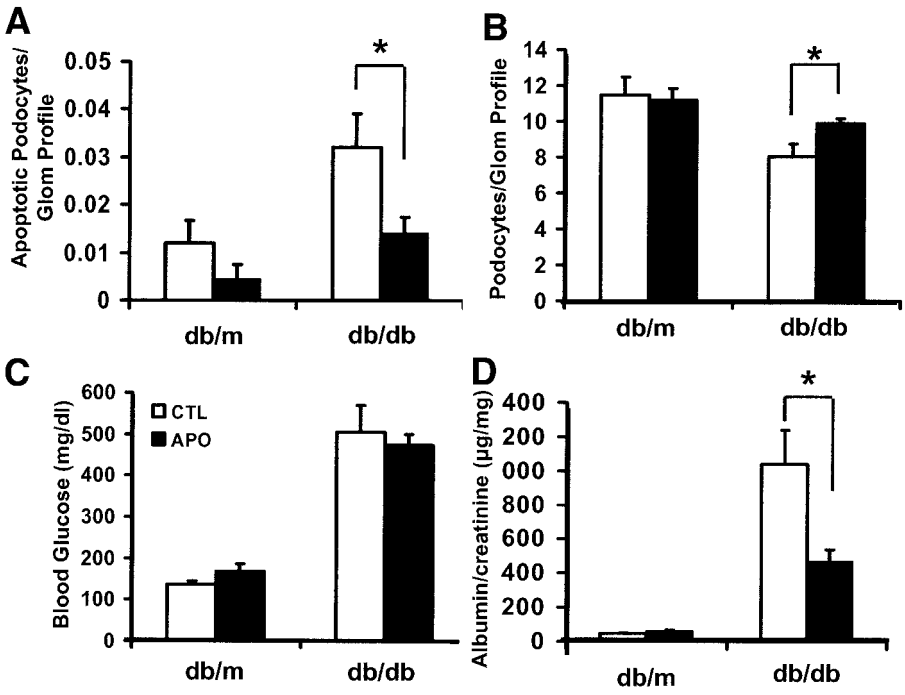

FIG. 6. Apocynin (NADPH oxidase inhibitor) blocks podocyte apoptosis and depletion in *db/db* diabetic mice. Bars indicate means ± SE of measurements of apoptotic podocytes per glomerular section (*A*), podocyte numbers per glomerular section (*B*), blood glucose levels (*C*), and urinary albumin-to-creatinine ratio (µg/mg) (*D*) in nondiabetic control *db/m* and diabetic *db/db* mice that were either untreated (□) or treated with apocynin in drinking water (■). Podocyte apoptosis (*A*) was analyzed at 8 weeks of age; all other measurements were obtained in 20-week-old mice. $n = 8$ mice/each genotype/each treatment group. *$P < 0.05$.

nephritis and in the TGF-β1 transgenic and the CD2AP knockout mouse models of glomerulosclerosis (20,21,37). In the last two models, we demonstrated that podocyte apoptosis is an early glomerular phenotype that coincides with onset of albuminuria and associated with progressive podocyte depletion. Mechanistic experiments with puromycin aminonucleoside administration to induce toxic podocyte injury and cell depletion in rats also provided experimental evidence that podocyte depletion is as an initiating event in glomerulosclerosis (38). Sclerosing glomeruli are characterized by progressive depletion of podocytes, resulting in denuded glomerular basement membrane areas and tuft adhesions that may be considered as initial lesions of irreversible glomerular injury (39). These studies suggest that podocyte apoptosis and depletion in nondiabetic models of glomerulosclerosis may be sufficient to trigger events leading to progressive glomerulosclerosis (40–44).

Our findings that podocyte apoptosis coincided with onset of hyperglycemia indicate that glucotoxicity may underlie the activation of proapoptotic signaling. Glucose has previously been shown to induce apoptosis in mesangial cells, in dorsal root ganglion cells, in cardiac myocytes, and possibly in renal tubular epithelial cells (30–32). However, the effects of high ambient glucose on podocytes have not been previously examined. Using a murine conditionally immortalized podocyte cell line (25), we demonstrated that glucose is sufficient to induce apoptosis starting a 20-mmol/l concentration. Consistent with the hypothesis of Brownlee and colleagues (45,46), high glucose stimulated rapid ROS generation in podocytes from mitochondrial and nonmitochondrial sources. In our

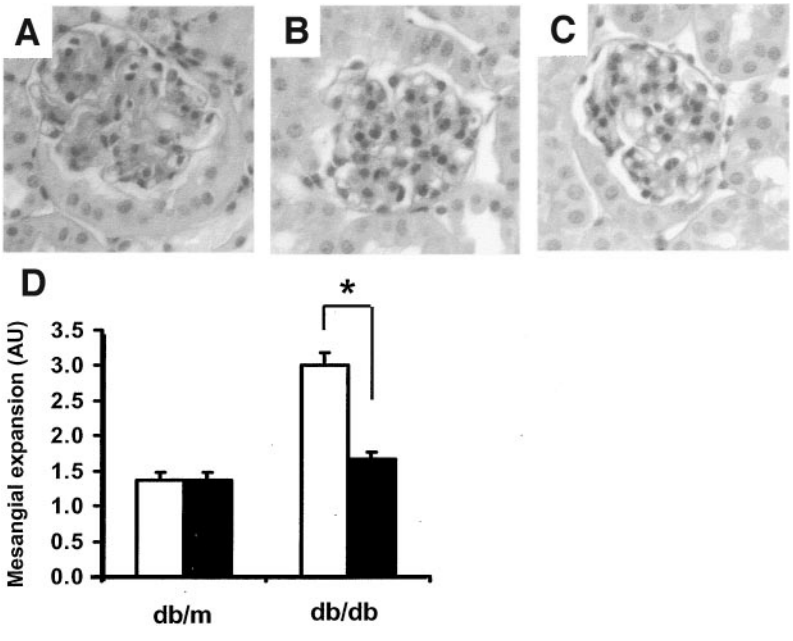

FIG. 7. Apocynin treatment blocks the development of mesangial expansion in *db/db* mice. *A–C*: PAS-stained kidney sections from 20-week-old control *db/db* (*A*), apocynin-treated *db/db* (*B*), and control *db/m* mice (*C*). *D*: Means ± SE of mesangial expansion scores in untreated (□) *db/m* and *db/db* mice and in apocynin-treated (■) *db/m* and *db/db* mice. $n = 8$ mice/each genotype/each treatment group. *$P < 0.05$.

study, the kinetic profile showed significant induction of ROS content as early as 0.5 h; this was followed by the activation of the proapoptotic p38 MAPK pathway after 2 h of exposure and effector caspase 3 activation after 3 h of incubation. A possible molecular link between ROS and MAPK activation was suggested by the observation that increased oxidative stress activates Jun NH_2-terminal kinase and p38 MAPK through apoptosis signal–regulating kinase 1 (47). Prior studies have linked the activation of p38 MAPK to podocyte apoptosis (20,48). Studies to delineate further the molecular pathway(s) of ROS-induced podocyte apoptosis are ongoing in our laboratory.

We may conclude that NADPH oxidase–dependent ROS generation constitutes a major pathway resulting in diabetes/glucose-induced podocyte apoptosis in vitro and in vivo. This was validated in principle in vivo after chronic NADPH oxidase inhibition in *db/db* mice. A role for NADPH oxidase has previously been suggested in the development of diabetic cardiovascular and renal complications (33,49). Blockade of NADPH oxidase over 12 weeks of diabetes significantly decreased but did not completely normalize urinary albumin excretion and podocyte depletion. These results indicate that NADPH oxidase–independent pathways (i.e., mitochondrial ROS generation and TGFβ [50]) might also contribute to diabetes-induced albuminuria and podocyte depletion in *db/db* mice. In addition, events other than apoptosis might also play a role in podocyte depletion. For example, detachment of viable podocytes has been suggested previously in a streptozotocin-induced diabetic model in rats and may contribute to podocyte loss (16,18). Moreover the effect of apocyanin on cells other than podocytes, might also contribute to its beneficial effects; therefore, new approaches to generate podocyte-selective inhibition of ROS-generating pathways will be required to resolve these questions definitively. Considering these limitations of the current study, our findings nevertheless demonstrate for the first time that ROS-mediated podocyte apoptosis represents an early glomerular cell defect associated with subsequent glomerulopathy in murine type 1 and type 2 diabetic models. This novel conclusion is highly significant because it may provide new approaches to prevention of diabetic nephropathy by targeting inhibition of ROS and apoptosis pathways, including NADPH oxidase and p38 MAPK.

ACKNOWLEDGMENTS

K.S. has received the National Kidney Foundation Young Investigator Award and the Juvenile Diabetes Research Foundation Career Development Award. M.S. has received a research fellowship of the Juvenile Diabetes Research Foundation and of the National Kidney Foundation. E.P.B. has received National Institutes of Health grants UO1DK060995, RO1DK056077, and RO1DK060043.

We thank Chih-Kang Huang and Alisha Biser for their technical support and Dr. Peter Mundel (Mount Sinai School of Medicine, NY) for providing the conditionally immortalized murine podocyte cell line. We thank Mr. John Basgen (University of Minnesota, Minneapolis, MN) for his assistance with the glomerular volume measurements.

Part of these results were presented at the Annual Scientific Meeting of the American Society of Nephrology, St. Louis, Missouri, 27 October to 1 November 2004.

REFERENCES

1. USRDS: the United States Renal Data System. *Am J Kidney Dis* 42:1–230, 2003
2. Drummond K, Mauer M: The early natural history of nephropathy in type 1 diabetes. II. Early renal structural changes in type 1 diabetes. *Diabetes* 51:1580–1587, 2002
3. Mauer M, Drummond K: The early natural history of nephropathy in type 1 diabetes. I. Study design and baseline characteristics of the study participants. *Diabetes* 51:1572–1579, 2002
4. Steinke JM, Sinaiko AR, Kramer MS, Suissa S, Chavers BM, Mauer M: The early natural history of nephropathy in type 1 diabetes. III. Predictors of 5-year urinary albumin excretion rate patterns in initially normoalbuminuric patients. *Diabetes* 54:2164–2171, 2005
5. Fioretto P, Steffes MW, Brown DM, Mauer SM: An overview of renal pathology in insulin-dependent diabetes mellitus in relationship to altered glomerular hemodynamics. *Am J Kidney Dis* 20:549–558, 1992
6. Danesh FR, Sadeghi MM, Amro N, Philips C, Zeng L, Lin S, Sahai A, Kanwar YS: 3-Hydroxy-3-methylglutaryl CoA reductase inhibitors prevent high glucose-induced proliferation of mesangial cells via modulation of Rho GTPase/ p21 signaling pathway: implications for diabetic nephropathy. *Proc Natl Acad Sci U S A* 99:8301–8305, 2002
7. Forbes JM, Thallas V, Thomas MC, Founds HW, Burns WC, Jerums G, Cooper ME: The breakdown of preexisting advanced glycation end products is associated with reduced renal fibrosis in experimental diabetes. *FASEB J* 17:1762–1764, 2003
8. Wendt T, Tanji N, Guo J, Hudson BI, Bierhaus A, Ramasamy R, Arnold B, Nawroth PP, Yan SF, D'Agati V, Schmidt AM: Glucose, glycation, and RAGE: implications for amplification of cellular dysfunction in diabetic nephropathy. *J Am Soc Nephrol* 14:1383–1395, 2003
9. The Diabetes Control and Complications Trial/Epidemiology of Diabetes Interventions and Complications Research Group: Retinopathy and nephropathy in patients with type 1 diabetes four years after a trial of intensive therapy. *N Engl J Med* 342:381–389, 2000
10. Colwell JA: Intensive insulin therapy in type II diabetes: rationale and collaborative clinical trial results. *Diabetes* 45 (Suppl. 3):S87–S90, 1996
11. Wolf G, Chen S, Ziyadeh FN: From the periphery of the glomerular capillary wall toward the center of disease: podocyte injury comes of age in diabetic nephropathy. *Diabetes* 54:1626–1634, 2005
12. Ziyadeh FN: Mediators of diabetic renal disease: the case for TGF-beta as the major mediator. *J Am Soc Nephrol* 15 (Suppl. 1):S55–S57, 2004
13. Ziyadeh FN, Sharma K: Overview: combating diabetic nephropathy. *J Am Soc Nephrol* 14:1355–1357, 2003
14. Pagtalunan ME, Miller PL, Jumping-Eagle S, Nelson RG, Myers BD, Rennke HG, Coplon NS, Sun L, Meyer TW: Podocyte loss and progressive glomerular injury in type II diabetes. *J Clin Invest* 99:342–348, 1997
15. Meyer TW, Bennett PH, Nelson RG: Podocyte number predicts long-term urinary albumin excretion in Pima Indians with type II diabetes and microalbuminuria. *Diabetologia* 42:1341–1344, 1999
16. Petermann AT, Krofft R, Blonski M, Hiromura K, Vaughn M, Pichler R, Griffin S, Wada T, Pippin J, Durvasula R, Shankland SJ: Podocytes that detach in experimental membranous nephropathy are viable. *Kidney Int* 64:1222–1231, 2003
17. Durvasula RV, Petermann AT, Hiromura K, Blonski M, Pippin J, Mundel P, Pichler R, Griffin S, Couser WG, Shankland SJ: Activation of a local tissue angiotensin system in podocytes by mechanical strain. *Kidney Int* 65:30–39, 2004
18. Vogelmann SU, Nelson WJ, Myers BD, Lemley KV: Urinary excretion of viable podocytes in health and renal disease. *Am J Physiol Renal Physiol* 285:F40–F48, 2003
19. Bottinger EP, Bitzer M: TGF-beta signaling in renal disease. *J Am Soc Nephrol* 13:2600–2610, 2002
20. Schiffer M, Bitzer M, Roberts IS, Kopp JB, ten Dijke P, Mundel P, Bottinger EP: Apoptosis in podocytes induced by TGF-beta and Smad7. *J Clin Invest* 108:807–816, 2001
21. Schiffer M, Mundel P, Shaw AS, Bottinger EP: A novel role for the adaptor molecule CD2-associated protein in transforming growth factor-beta-induced apoptosis. *J Biol Chem* 279:37004–37012, 2004
22. Cotter MA, Cameron NE: Effect of the NAD(P)H oxidase inhibitor, apocynin, on peripheral nerve perfusion and function in diabetic rats. *Life Sci* 73:1813–1824, 2003
23. Beswick RA, Dorrance AM, Leite R, Webb RC: NADH/NADPH oxidase and enhanced superoxide production in the mineralocorticoid hypertensive rat. *Hypertension* 38:1107–1111, 2001
24. Park YM, Park MY, Suh YL, Park JB: NAD(P)H oxidase inhibitor prevents blood pressure elevation and cardiovascular hypertrophy in aldosterone-infused rats. *Biochem Biophys Res Commun* 313:812–817, 2004

25. Mundel P, Heid HW, Mundel TM, Kruger M, Reiser J, Kriz W: Synaptopodin: an actin-associated protein in telencephalic dendrites and renal podocytes. *J Cell Biol* 139:193–204, 1997
26. Breyer MD, Bottinger E, Brosius FC III, Coffman TM, Harris RC, Heilig CW, Sharma K: Mouse models of diabetic nephropathy. *J Am Soc Nephrol* 16:27–45, 2005
27. Susztak K, Sharma K, Schiffer M, McCue P, Ciccone E, Bottinger EP: Genomic strategies for diabetic nephropathy. *J Am Soc Nephrol* 14:S271–S278, 2003
28. Sharma K, McCue P, Dunn SR: Diabetic kidney disease in the db/db mouse. *Am J Physiol Renal Physiol* 284:F1138–F1144, 2003
29. Susztak K, Ciccone E, McCue P, Sharma K, Bottinger EP: Multiple metabolic hits converge on CD36 as novel mediator of tubular epithelial apoptosis in diabetic nephropathy. *PLoS Med* 2:e45, 2005
30. Kang BP, Frencher S, Reddy V, Kessler A, Malhotra A, Meggs LG: High glucose promotes mesangial cell apoptosis by oxidant-dependent mechanism. *Am J Physiol Renal Physiol* 284:F455–F466, 2003
31. Vincent AM, McLean LL, Backus C, Feldman EL: Short-term hyperglycemia produces oxidative damage and apoptosis in neurons. *FASEB J* 19:638–640, 2005
32. Fiordaliso F, Leri A, Cesselli D, Limana F, Safai B, Nadal-Ginard B, Anversa P, Kajstura J: Hyperglycemia activates p53 and p53-regulated genes leading to myocyte cell death. *Diabetes* 50:2363–2375, 2001
33. Asaba K, Tojo A, Onozato ML, Goto A, Quinn MT, Fujita T, Wilcox CS: Effects of NADPH oxidase inhibitor in diabetic nephropathy. *Kidney Int* 67:1890–1898, 2005
34. Greiber S, Munzel T, Kastner S, Muller B, Schollmeyer P, Pavenstadt H: NAD(P)H oxidase activity in cultured human podocytes: effects of adenosine triphosphate. *Kidney Int* 53:654–663, 1998
35. Susztak K, Bottinger E, Novetsky A, Liang D, Zhu Y, Ciccone E, Wu D, Dunn S, McCue P, Sharma K: Molecular profiling of diabetic mouse kidney reveals novel genes linked to glomerular disease. *Diabetes* 53:784–794, 2004
36. Steffes MW, Schmidt D, McCrery R, Basgen JM: Glomerular cell number in normal subjects and in type 1 diabetic patients. *Kidney Int* 59:2104–2113, 2001
37. Pippin JW, Durvasula R, Petermann A, Hiromura K, Couser WG, Shankland SJ: DNA damage is a novel response to sublytic complement C5b-9-induced injury in podocytes. *J Clin Invest* 111:877–885, 2003
38. Kim YH, Goyal M, Kurnit D, Wharram B, Wiggins J, Holzman L, Kershaw D, Wiggins R: Podocyte depletion and glomerulosclerosis have a direct relationship in the PAN-treated rat. *Kidney Int* 60:957–968, 2001
39. Rennke HG: How does glomerular epithelial cell injury contribute to progressive glomerular damage? *Kidney Int Suppl* 45:S58–S63, 1994
40. Kriz W: Progression of chronic renal failure in focal segmental glomerulosclerosis: consequence of podocyte damage or of tubulointerstitial fibrosis? *Pediatr Nephrol* 18:617–622, 2003
41. Kriz W: Evolving role of the podocyte in chronic renal failure. *Kidney Blood Press Res* 20:180–183, 1997
42. Kriz W, Gretz N, Lemley KV: Progression of glomerular diseases: is the podocyte the culprit? *Kidney Int* 54:687–697, 1998
43. Kriz W, Lemley KV: The role of the podocyte in glomerulosclerosis. *Curr Opin Nephrol Hypertens* 8:489–497, 1999
44. Pavenstadt H, Kriz W, Kretzler M: Cell biology of the glomerular podocyte. *Physiol Rev* 83:253–307, 2003
45. Brownlee M: Biochemistry and molecular cell biology of diabetic complications. *Nature* 414:813–820, 2001
46. Nishikawa T, Edelstein D, Du XL, Yamagishi S, Matsumura T, Kaneda Y, Yorek MA, Beebe D, Oates PJ, Hammes HP, Giardino I, Brownlee M: Normalizing mitochondrial superoxide production blocks three pathways of hyperglycaemic damage. *Nature* 404:787–790, 2000
47. Goldman EH, Chen L, Fu H: Activation of apoptosis signal-regulating kinase 1 by reactive oxygen species through dephosphorylation at serine 967 and 14-3-3 dissociation. *J Biol Chem* 279:10442–10449, 2004
48. Koshikawa M, Mukoyama M, Mori K, Suganami T, Sawai K, Yoshioka T, Nagae T, Yokoi H, Kawachi H, Shimizu F, Sugawara A, Nakao K: Role of p38 mitogen-activated protein kinase activation in podocyte injury and proteinuria in experimental nephrotic syndrome. *J Am Soc Nephrol* 16:2690–2701, 2005
49. Hayashi T, Juliet PA, Kano-Hayashi H, Tsunekawa T, Dingqunfang D, Sumi D, Matsui-Hirai H, Fukatsu A, Iguchi A: NADPH oxidase inhibitor, apocynin, restores the impaired endothelial-dependent and -independent responses and scavenges superoxide anion in rats with type 2 diabetes complicated by NO dysfunction. *Diabetes Obes Metab* 7:334–343, 2005
50. Ziyadeh FN, Hoffman BB, Han DC, Iglesias-De La Cruz MC, Hong SW, Isono M, Chen S, McGowan TA, Sharma K: Long-term prevention of renal insufficiency, excess matrix gene expression, and glomerular mesangial matrix expansion by treatment with monoclonal antitransforming growth factor-beta antibody in db/db diabetic mice. *Proc Natl Acad Sci U S A* 97:8015–8020, 2000